Construction of Functional Biomaterials by Biomolecular Self-assembly

Kazunori Matsuura*

Department of Chemistry and Biotechnology, Graduate School of Engineering, Tottori University, Tottori 680-8552, Japan.

E-mail: < ma2ra-k@chem.tottori-u.ac.jp.>

Kazunori Matsuura

Kazunori Matsuura obtained his Ph.D. from Tokyo Institute of Technology in 1996. In 1996, he joined the Department of Molecular Design and Engineering, Nagoya University, as an Assistant Professor. In 2001, he moved to the Department of Chemistry and Biochemistry, Kyushu University, as an Associate Professor. In 2006, he was selected as a researcher for the JST PRESTO project "Structure Control and Function." In 2012, he moved to the Department of Chemistry and Biotechnology, Tottori University, as a full Professor.

Abstract

This account discusses construction strategies for various functional biomaterials based on the designed self-assembly of biomolecules. Novel glycoclusters with regular intervals were developed by self-assembly of carbohydrate-conjugated oligodeoxyribonucleotides (ODNs) with the half-sliding complementary ODNs. Complexes of carbohydrate-modified DNA and lectin afforded a new regulation system for gene expression. DNA three-way junctions bearing self-complementary sticky-ends were self-assembled into nanometer-to-micrometer-sized spherical structures depending on the concentration. The three-way component design was extended to the design of an artificial trigonal peptide conjugate. The trigonal peptide conjugates bearing β-sheet–forming peptides or glutathione self-assembled into nano-sized spherical assemblies. Self-assembly of β-annulus peptide derived from tomato bushy stunt virus afforded artificial viral capsids, which can encapsulate and be modified with various molecules.

1. Introduction

In biological systems, nano- and micron-sized biological supramolecules with various functions are formed spontaneously by self-assembly of biomolecules such as proteins and nucleic acids.[1] For example, the chromatin structure is a beads-on-strings structure self-assembled from nucleic acids and histone proteins in the nucleus. Viruses comprise genome nucleic acids encapsulated in outer protein shells with a discrete size known as capsids, which are self-assembled from proteins. Microtubules are natural nanotubes self-assembled from tubulin α and β in the presence of GTP, which participates in the formation of cytoskeleton. Clathrin lattice is a polyhedral structure self-assembled from triskelion comprising three proteins in the presence of Mg^{2+}, which participates in receptor-mediated endocytosis. Establishing a methodology for artificially constructing nano-/micro-structures learned from biological self-assembly strategies can contribute greatly to the development of bottom-up nanotechnology. Although artificial amphiphilic molecules self-assemble into micelles and vesicles, as known since long ago, it is difficult to construct the complex and precise bio-supramolecules described above only by amphipathic molecular design. In the past 20 years, molecular designs for constructing nano-/micro-structures with a desired size, shape, and function in a bottom-up manner have been developed by utilizing regular secondary structure formation of DNA and peptides/proteins and mimicking biological supramolecular formation.[2-5] The advantages of constructing nano-/micro-structures are that they have a relatively rigid conformation, so that secondary structure formation can be predicted from the primary sequence and self-assembly can be programmed. In addition, there is an advantage for their excellent biocompatibility. From such a viewpoint, the author's research group has been studying ways of constructing nanostructured systems comprising biomolecules by mimicking self-assembly strategies in vivo. This account discusses our research into the construction of nano-/micro-sized biomolecular systems self-assembled from rationally designed DNA and peptides.

2. Spatial Arrangement of Carbohydrates via DNA Hybridization

Oligosaccharide chains present as glycolipids or glycoproteins on the cell surface are important biomolecules involved in various physiological phenomena such as cell adhesion, intercellular communication, and virus infection. Molecular recognition of oligosaccharides by lectins (oligosaccharide-binding proteins) is known to increase as the oligosaccharides become denser, which is called the "multivalent effect" or the "glycocluster effect."[6-9] So far, artificial glycoclusters based on synthetic polymers showing such a multivalent glycocluster effect have been developed, not only as a model of molecular recognition involving glycolipids and glycoproteins but also as a cell culture substrate, material for trapping viruses and toxins, sensing material, drug delivery material, and regulating material of amyloid fibrils.[9] In densely arranged glycoclusters based on synthetic homopolymers such as polystyrene and polyacrylamide as the main chain, the lectin-recognizing ability may decrease due to steric hindrance in some cases.[10] Although copolymerization can space the oligosaccharides on average intervals, it is difficult to synthesize macromolecules in which the intervals of oligosaccharides are regularly controlled (Figure 1A).

Since DNA double helix has a relatively rigid conformation and regular helical pitch, it is promising as a scaffold for arranging functional molecules at regular intervals. Ohya and co-workers demonstrated sequential fluorescence energy transfer among dyes that were arranged along an assembly comprising dye-modified oligodeoxyribonucleotide (ODN) and template ODN.[11] In 2001, we applied the strategy of aligning functional molecules along DNA duplex for the first time in molecular recognition, and succeeded in obtaining a one-dimensional arrangement of galactoses with a regular interval by DNA hybridization (Figure 2B).[12-16] Galactose-modified ODNs were synthesized by solid-phase phosphoramidite chemistry using a 5'-β-galactoside-modified deoxyuracil derivative, which was synthesized via Sonogashira coupling.[12] A self-assembled

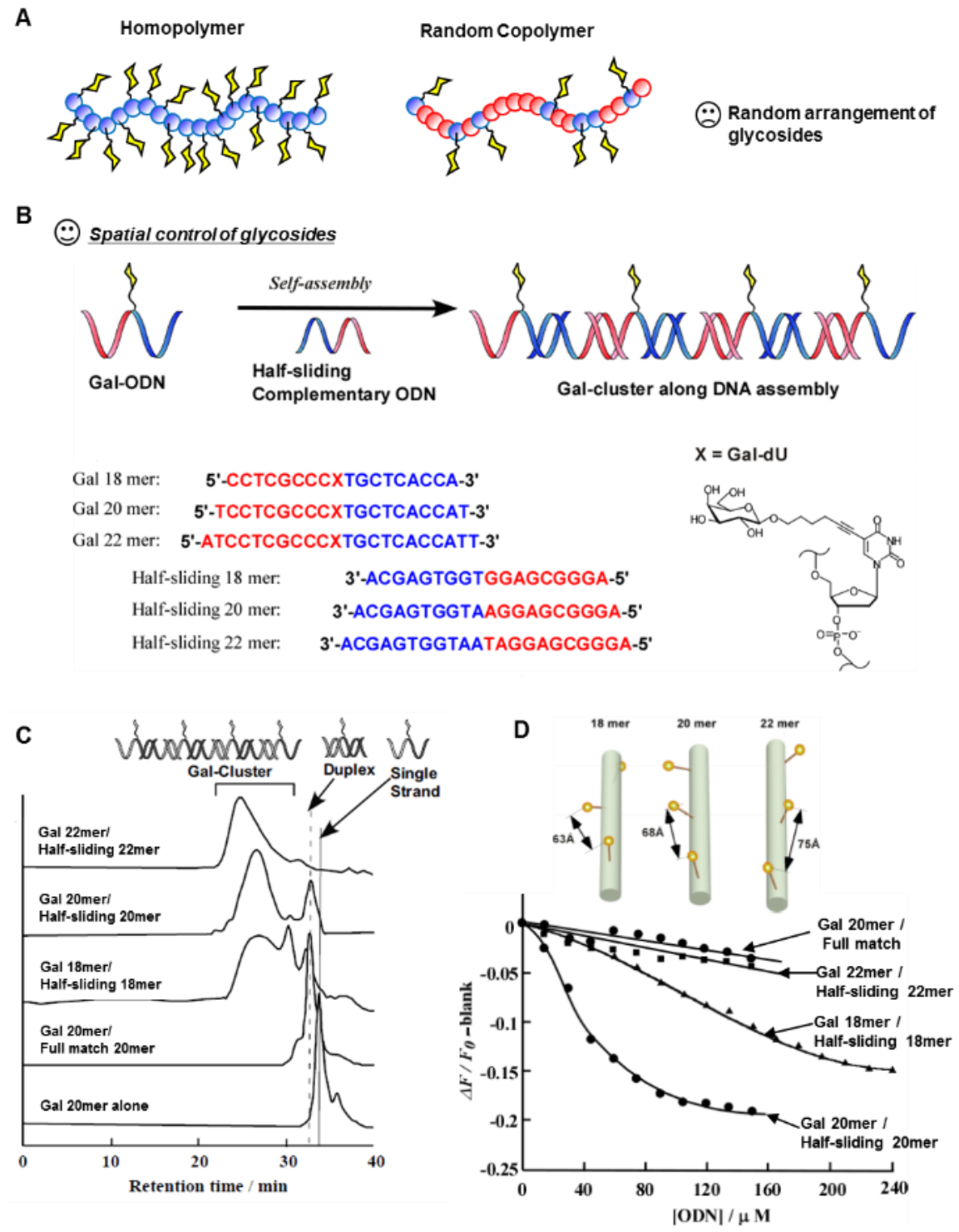

Figure 1. (A) Artificial glycoclusters based on synthetic polymers. (B) *β*-Gal-cluster along double-strand DNA self-assembled from galactosylated ODN with the half-sliding complementary ODN. (C) Size-exclusion chromatograph of galactosylated ODNs. (D) Dependence of fluorescence intensity of FITC-RCA_{120} at 520 nm (Ex = 490 nm) on the concentration of ODNs in PBS (pH 7.4) at 25 ºC.

β-Gal-cluster along double-strand DNA was constructed by hybridization of *β*- galactoside-modified ODN (*β*-Gal-ODN) and the half-sliding complementary ODN (hscODN).[13, 14] Because the B-type DNA duplex had 10.5 base pairs and 3.4-nm pitch per helical turn, *β*-Gal residues were displayed at 6.8 nm intervals with a small dihedral angle by hybridization of 20-mer *β*-Gal-ODN and the 20-mer hscODN. Size-exclusion chromatography (SEC) of 18-mer, 20-mer, and 22-mer *β*-Gal-ODN/hscODN duplexes was shifted to faster retention times than those of the single-strand ODN alone and the full complementary duplex, suggesting the formation of *β*-Gal-cluster by hybridization (Figure 2C).

RCA_{120}, one of the galactose-recognizing lectins, has four binding sites that are about 6.5 nm apart. Figure 2D shows the concentration dependence of *β*-Gal-clusters along the ODN assembly on the binding to FITC-labeled RCA_{120}. The self-assembled *β*-Gal cluster with 6.8 nm intervals along the 20-mer *β*-Gal-ODN/hscODN duplex was strongly and cooperatively

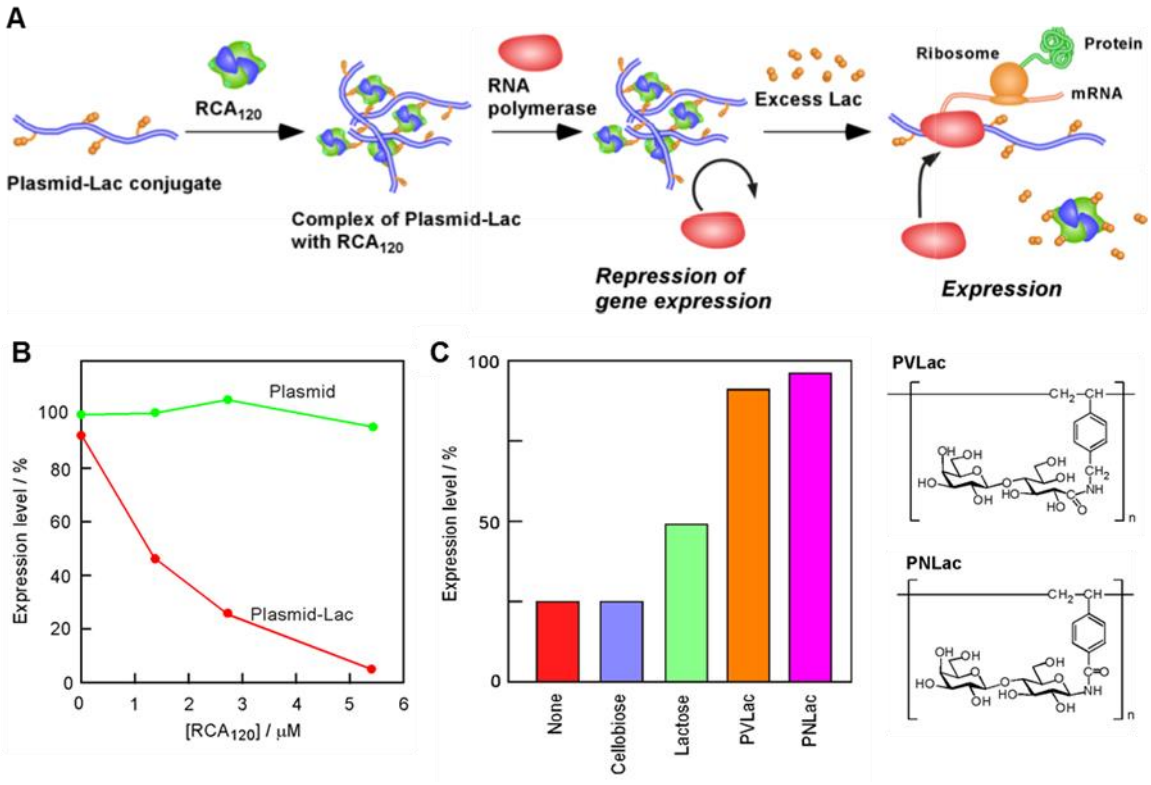

Figure 2. (A) Schematic illustration of a model system for regulation of gene expression utilizing carbohydrate–lectin interactions. (B) Dependence of repression of expression activity of Lac-modified pGFP on RCA_{120} concentration. (C) Recovery of the repressed expression activity of Lac-modified pGFP by adding lactose derivatives.

bound to RCA_{120} lectin ($K_a = 5.5 \times 10^4\ M^{-1}$, $n = 2.4$). In contrast, the largely twisted β-Gal-cluster with 6.3 nm intervals based on the 18-mer β-Gal-ODN/hscODN duplex was more weakly and less cooperatively bound ($K_a = 1.9 \times 10^4\ M^{-1}$ and $n = 1.8$), and the 22-mer β-Gal-cluster with an extended interval was not bound to RCA_{120}. These results indicate that when the spatial arrangement of the β-Gal cluster fits the binding sites of RCA_{120}, they strongly and cooperatively bind to lectin. Therefore, we succeeded in controlling the lectin-recognizing ability by controlling the arrangement of β-Gals using ODN as a molecular ruler. In the same way, the affinity of α-mannoside-modified ODN for concanavalin A lectin was amplified by hybridization with the hscODN.[15] We also demonstrated that the affinity of glycopolymer-ODN conjugate carrying α-mannosides for Con A was increased about 2 times by hybridization with the hscODN.[16]

Inspired by our research, Seitz and coworkers demonstrated that oligosaccharide-displayed peptide nucleic acid (PNA)–ODN complexes were useful for the spatial screening of oligosaccharide–lectin interactions.[17, 18] They also demonstrated that bivalent peptide-displayed duplexes with regular intervals as molecular rulers effectively bound to tandem SH2 domain of Syk kinase.[19] Moreover, Montesarchio and coworkers reported antiviral activity against HIV-1 of glycoconjugated DNA quadruplex.[20] Hamilton and coworkers constructed a pentaplex assembly of phosphocholine (PC)–DNA conjugate in the presence of Cs^+ ions and revealed that the pentaplex assembly of PC binds to human C-reactive protein with 350-fold higher affinity than its monomeric counterpart.[21] Ebara and coworkers demonstrated that glycoclusters displayed on three-way junction DNA bound to lectins with higher affinity than those along linear dsDNA.[22]

3. Regulation of Gene Expression using Assemblies via Carbohydrate–Lectin Interaction

In eukaryotes, DNA is packaged in a nucleus as chromatin by interaction with histone proteins, in which gene expression is usually repressed. When "chromatin remodeling" such as acetylation of histones occurs, the gene expression is turned on. Artificial on–off switching of gene expression is important in synthetic biology, especially for medical applications. Asanuma and coworkers developed an artificial photo-responsive regulation system of transcription using an azobenzene-modified promoter.[23] Katayama and coworkers developed phosphorylation signal-responsive artificial gene regulation system using polymers carrying oligopeptides.[24]

In 2002, we developed a novel strategy for an artificial on–off switching system of gene expression by applying the recognition of plasmid–lactose conjugate to lectin (Figure 2).[25, 26] Conjugates of plasmid DNAs with lactose were prepared by diazo-coupling with a diazonium derivative of lactose.[27, 28] Interestingly, the plasmid–lactose conjugate retained the transcription activity, despite the existence of nucleotides modified with lactose. When the plasmid–lactose conjugate was complexed strongly with RCA_{120} lectin, access of RNA polymerase to the template DNA was hindered and the transcription of DNA was repressed. When an excess amount of lactose or lactose-carrying polymer were added to the complex, the binding between the plasmid–lactose conjugate and lectin was relaxed, and RNA polymerase became accessible to the DNA to recover the transcription (Figure 2A). Agarose gel-shift assay of the plasmid–lactose conjugate (lactose content = 8.2% per base) revealed that the conjugate was specifically recognized by RCA_{120} lectin with the strong affinity constant $K_a = 7.6 \times 10^5\ M^{-1}$ per Lac unit. TEM and AFM images showed that aggregates of submicron to micron size were formed by the interaction

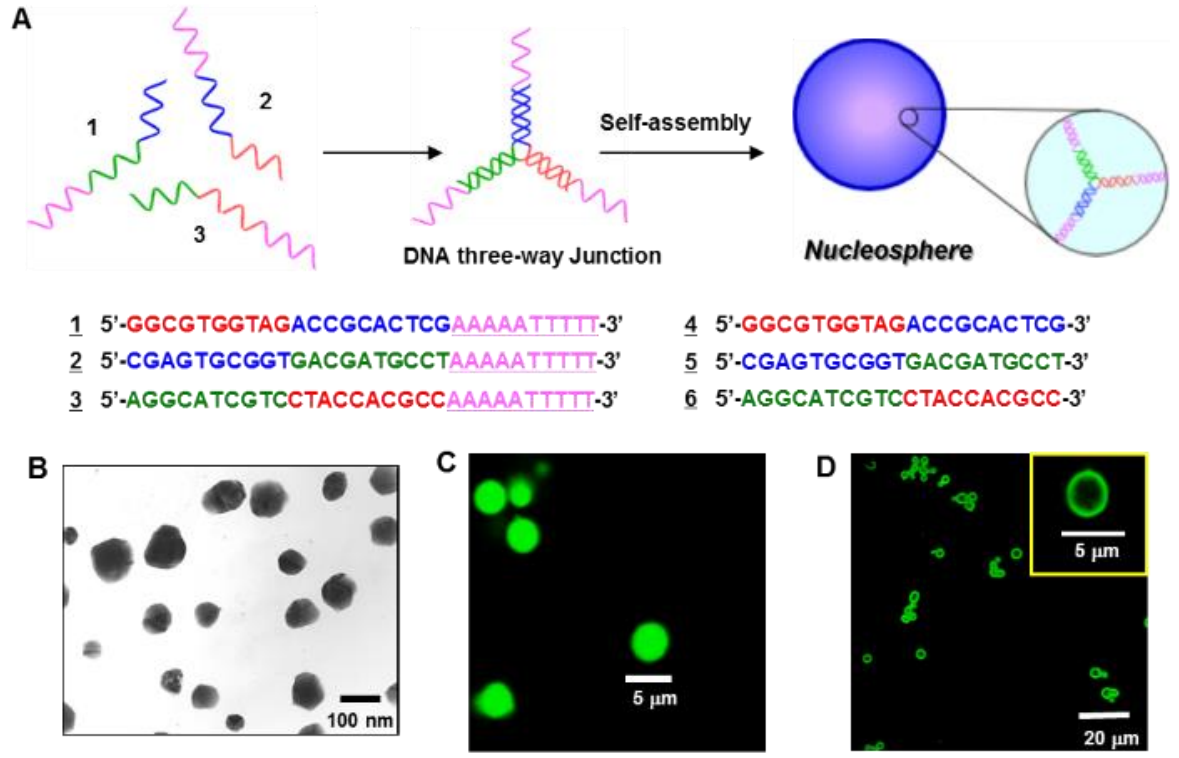

Figure 3. (A) Schematic illustration of the formation of nucleo-spheres by self-assembly of DNA three-way junctions bearing self-complementary sticky ends. (B) TEM image of nucleo-spheres comprising ODNs **1–3** at $[ODN]_{total}$ = 5 μM. (C) CLSM image of nucleo-spheres comprising ODNs **1–3** at $[ODN]_{total}$ = 20 μM in the presence of 1 μM YOYO-1. (D) CLSM image of hollow nucleo-spheres induced by addition of cationic surfactant.

between the conjugate and lectin. Figure 2B shows the dependence of RCA_{120} concentration on the *in vitro* expression level of pGFP–lactose conjugate (lactose content = 8.7% per base), which was estimated from the fluorescence intensity at 507 nm. The expression level of pGFP–lactose conjugate decreased with increasing concentration of RCA_{120}, whereas that of unmodified pGFP was not affected by RCA_{120}. When an excess amount of lactose (1 mM) was added to the complex ([plasmid] = 76 nM, $[RCA_{120}]$ = 2.7 μM), approximately 50% of the expression was recovered, whereas the addition of 1 mM cellobiose did not affect the expression (Figure 2C). The addition of lactose-carrying polymers resulted in almost complete recovery of expression to the level of the pGFP–lactose conjugate in the absence of RCA_{120}. We propose a novel strategy for the artificial regulation of gene expression through carbohydrate–lectin interactions. The present system can be widely applied to the design of specific ligand-receptor-responding gene-expression systems.

4. Nucleo-spheres Self-assembled from DNA Three-way Junction

Since Seeman reported pioneering work on the construction of DNA cubes 10 nm in size in 1991, "DNA nanotechnology" research on nanostructure construction by DNA self-assembly has attracted much attention.[29, 30] DNA nanostructures termed "DNA origami" with a complex geometry were constructed by folding the long single-strand M13 phage DNA with short programed staple DNA, and are making rapid progress.[31, 32]

In 2003, we developed nano- and micron-sized spherical DNA assemblies, "nucleo-spheres," which consists of the simplest building blocks among the three-dimensional DNA nanostructures reported.[33-37] ODN **1**, **2**, and **3** were designed to form a DNA three-way junction bearing self-complementary sticky-ends (A_5T_5) and self-assemble into nucleo-spheres to consume all of the sticky-ends (Figure 3A). Three ODNs (**1**, **2**, and **3**) were mixed in a 1:1:1 molar ratio in 0.5 M NaCl aqueous solution at 25 °C, heated at 70 °C, and cooled slowly to 10 °C to construct nucleo-spheres. TEM images at a total ODN concentration of 5 μM showed the formation of spherical DNA assemblies of 50–150 nm in size (Figure 3B).[33] Neither an equimolar mixture of ODNs (**4**, **5**, and **6**), which lacks the self-complementary sticky-ends, nor a mixture of two ODNs out of the three (**1**, **2**, and **3**) produced spherical assemblies. The spherical assemblies were not digested by mung bean nuclease (a single-strand-specific endonuclease) and exonuclease III (a double-strand-specific 3′ to 5′ exonuclease), which indicates that the single- and double-strand terminal structures are absent on the spherical assemblies, providing evidence for the closed spherical structure.

The size of the nucleo-sphere became larger depending on the total nucleic acid concentration. At a total concentration of 20 μM, nucleo-spheres with a size of about 3–5 μm were observed in water by confocal laser scanning fluorescence microscopy (CLSM) when stained with YOYO-1, which is a DNA duplex-specific fluorescence probe (Figure 3C).[34, 35] This is a first example of micron-size DNA assemblies observed by CLSM. The fluorescence profile of one nucleo-sphere showed high fluorescence intensity even inside the assembly, suggesting that the interior is filled with DNA and the assemblies are not hollow structures. Interestingly, upon addition of a cationic surfactant such as cetyltrimethylammonium bromide (CTAB), nucleo-spheres underwent an unexpected dynamic transformation from filled spheres into hollow capsules (Figure 3D).[36] The morphological transition of nucleo-spheres might arise from the formation of multi-lamellar structures comprising

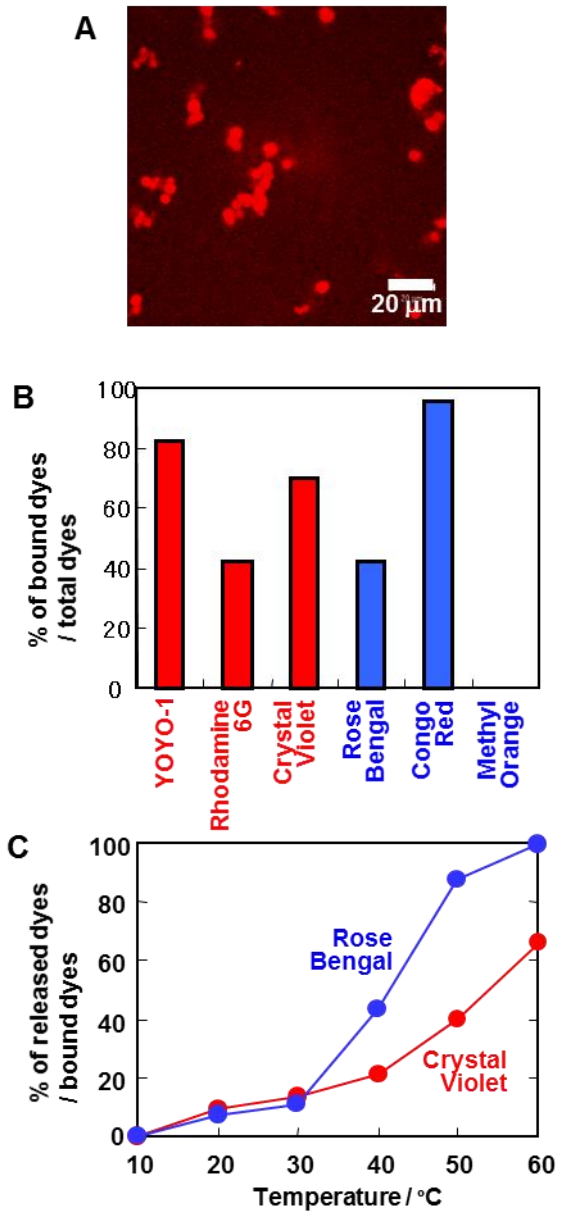

Figure 4. (A) CLSM image of nucleo-spheres formed in the presence of 100 μM Rose Bengal. (B) Population of dyes bound to nucleo-spheres relative to the total amount of dye. (C) Effect of temperature on the controlled release of Rose Bengal and Crystal Violet from nucleo-spheres.

a double-stand DNA-CTAB polyion complex at the surface of the nucleo-spheres.

When nucleo-spheres were constructed in the presence of a polarity-sensitive fluorophore (ANS), the CLSM image showed blue fluorescent spheres. The fluorescence intensity of ANS in the nucleo-sphere is increased 8-fold compared with ANS in pure water, indicating that the interior of the nuleo-spheres provides medium micropolarity (corresponding to an E_T^N value of 0.72). Therefore, even an anionic dye Rose Bengal, which hardly binds to DNA, can be effectively included into the nucleo-spheres by hydrophobic interactions (Figure 4A).[35] As shown in Figure 4B, not only cationic dyes (Rhodamine 6G, Crystal Violet, and YOYO-1) but also some anionic dyes (Rose Bengal and Congo Red) were strongly bound to the nucleo-spheres. Although spontaneous release of dyes in the nucleo-spheres was hardly observed at 25 °C after a long time, anionic Rose Bengal was effectively released from nulceo-spheres at 40–60 °C, corresponding to the melting temperature of the nucleo-spheres (Figure 4C). Thus, the nucleo-spheres can be expected to find use as a novel biomaterial for thermo-responsive drug delivery systems.

The nucleo-spheres can be modified with oligosaccharides by photoreaction with a psoralen-derivative-bearing lactose.[37] The binding of rhodamine-labeled peanut lectin (Rho-PNA) to lactose-displayed nucleo-spheres showed a relatively high binding constant on the order of 10^5 M^{-1}. CLSM observation revealed that the fluorescence of Rho-PNA was also detected from the inside of the lactose-displayed nucleo-sphere, not only from the surface, indicating that Rho-PNA is not only bound to the surface but also penetrates into the interior of the nucleo-spheres. These results suggest that nucleo-spheres possess pores in which proteins can penetrate, which could be exploited to create protein-trapping materials by employing appropriate ligand display.

5. Peptide Nanospheres Self-assembled from Trigonal Peptide Conjugates

Although the development of DNA nanotechnology is remarkable, applying diverse functions to the surface of DNA assemblies might be restricted because of the anionic charges of DNA, whereas diverse surface functions can be designed on peptide/protein assemblies. In the past decade, the construction of nano-architectures self-assembled from rationally designed peptides/proteins has been actively studied.[38-41] Using specific ligand-receptor interactions and secondary structures such as coiled-coils and β-sheets allows the design of precise and discrete peptide/protein assemblies such as fibers, tubes, rings, cages, and more complex structures.[38] For example, Wagner and coworkers have constructed a nanoring structure with a diameter of 8–20 nm by the interaction between dihydrofolate reductase dimer and a dimeric inhibitor.[42] Yeates and coworkers succeeded in constructing polyhedral protein nanostructures by self-assembling a fusion protein linking a dimerization protein subunit and a trimerization protein subunit.[43-45]

Since 2005, we have been studying the construction of virus-like nanostructures from peptides designed by mimicking the self-assembly strategy of natural viral capsids.[46-49] Spherical viral capsids with icosahedral symmetry include C_3-symmetry axes, and spherical clathrin is self-assembled from trigonal protein subunits. Mimicking these self-assembly strategies, we designed and synthesized a C_3-symmetric β-sheet-forming peptide conjugate, Trigonal-$(FKFE)_2$ (Figure 5A).[46] CD and FT-IR spectra showed that Trigonal-$(FKFE)_2$ adopts an antiparallel β-sheet structure. Scanning electron microscopy (SEM) and dynamic light scattering (DLS) measurements of Trigonal-$(FKFE)_2$ showed the formation of spherical assemblies with diameters of 19 ± 4 nm (Figure 5B, C), which is comparable to the estimated diameter of a dodecahedron structure (about 16 nm) formed via intermolecular antiparallel β-sheets. In contrast, the component peptide CFKFEFKFE afforded fibrous assemblies. The absence of fibrous assemblies from Trigonal-$(FKFE)_2$ indicates that the three-armed molecules self-assemble into a finite set of closed aggregates, most likely a dodecahedral structure comprising antiparallel β-sheets.

Next, we synthesized a C_3-symmetric peptide conjugate (Trigonal-WTW) bearing three tryptophan zipper-forming peptides (CKTWTWTE), and detected pH-dependent changes in the secondary structure and nanostructure of Trigonal-WTW in water.[48] The conjugate self-assembled into nanospheres about 30 nm in size via formation of a tryptophan zipper at pH 7, but into a mixture of nanofibers and nanospheres via formation of β-sheets at pH 11, and irregular aggregates via random coil

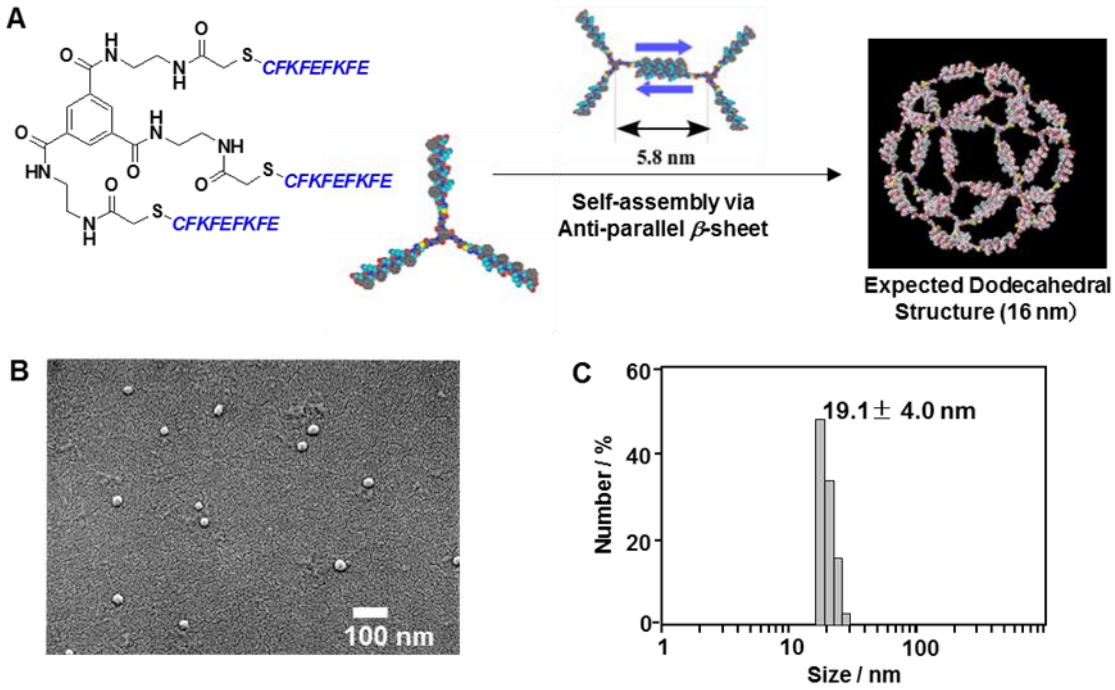

Figure 5. (A) Schematic illustration of the self-assembly of C_3-symmetric β-sheet-forming peptide conjugate, Trigonal-$(FKFE)_2$. (B) SEM image of spherical assemblies of Trigonal-$(FKFE)_2$. (C) Size distribution of the assemblies obtained from DLS.

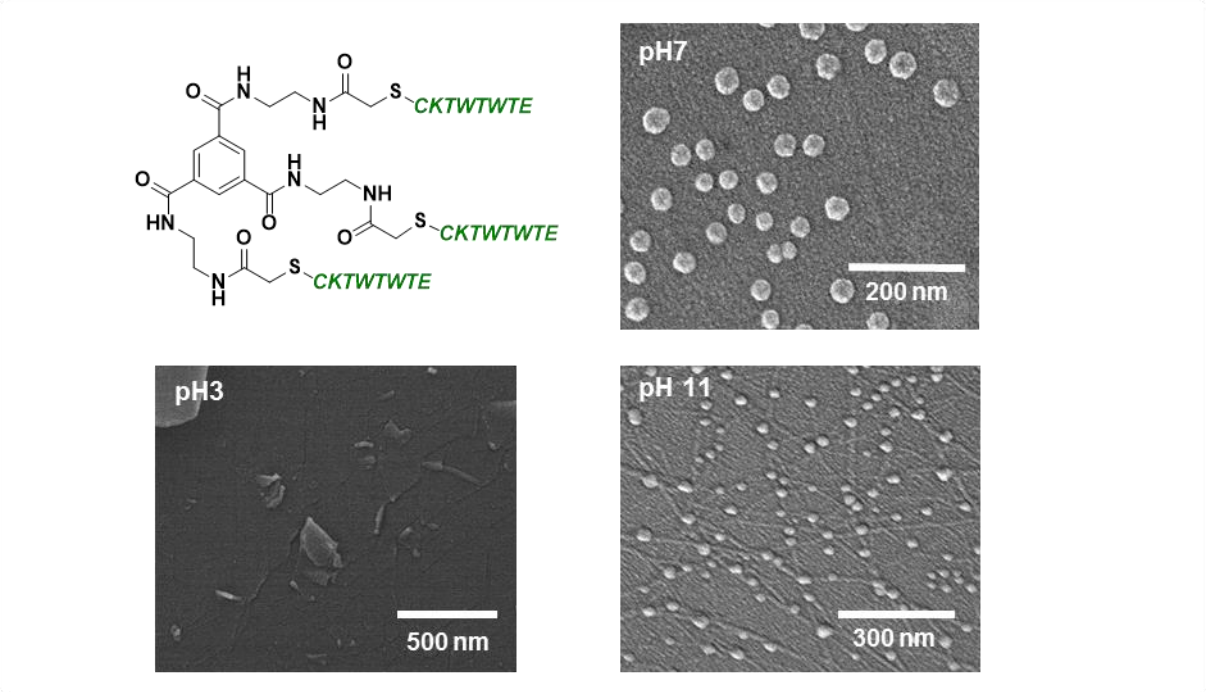

Figure 6. pH-Dependent self-assembly of C_3-symmetric tryptophan zipper-forming peptide conjugate, Trigonal-WTW.

structures at pH 3 (Figure 6). In contrast, the trigonal conjugate of CKTFTFTE, in which W is replaced by F, did not give a spherical structure regardless of pH. Thus, the formation of pH-dependent spherical structures is characteristic for trigonal conjugates of tryptophan zipper-forming peptides.

It has been reported that even short peptides such as dipeptides and tripeptides function as self-assembly units. Atkins and coworkers reported that oxidized glutathione formed fibrous assemblies in organic solvents to become an organogel.[50] In 2009, we found that trigonal conjugation of glutathione forms spherical assemblies with sizes of 100–250 nm in water (Figure 7A).[51] The SEM image of 1 mM trigonal glutathione (TG) shows the formation of wrinkly collapsed spherical assemblies, suggesting the existence of a hollow interior. Some guest molecules such as uranine and Methyl Orange were encapsulated into the TG nanosphere. When dithiothreitol

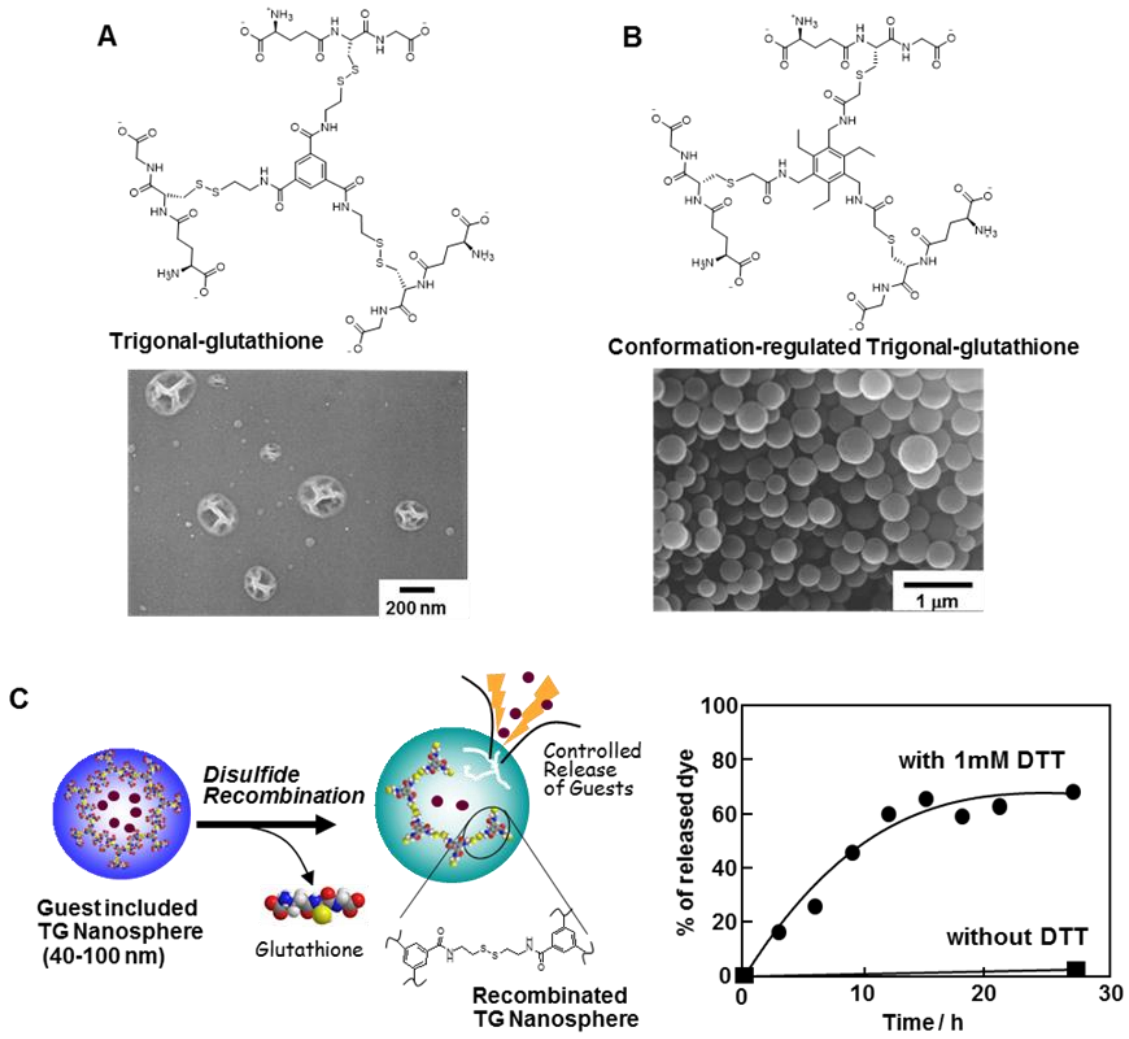

Figure 7. Self-assembly of trigonal-glutathione (A) and conformation-regulated trigonal-glutathione (B). (C) Controlled release of Methyl Orange from spherical assembly of trigonal-glutathione by disulfide recombination.

(DTT) was added to the guest-encapsulated TG nanospheres as a reducing agent, recombination of disulfide bonds occurred, glutathione was released while maintaining the nanosphere structure, and as a result, guest molecules were gradually released (Figure 7C).[52] In order to construct more regular nano-assemblies from glutathione derivatives, 1, 3, 5-tris(aminomethyl)-2, 4, 6-triethylbenzene was employed as the core of a new TG (Figure 7B).[53] The glutathione arms on the 1, 3,5-positions were assembled on one side of the scaffold due to the alternative conformation of the core. The conformation-regulated trigonal glutathione self-assembled into hard spherical structures with sizes of 310 ± 50 nm, which had regular morphologies and enhanced rigidity compared with those formed from conformationally non-regulated trigonal glutathione (Figure 7B).

The molecular strategy of "trigonal peptide conjugate" was extended to the construction of other self-assembling nanocapsules. Gazit and coworkers reported that trigonal dipeptide WW conjugate self-assembled into nanocapsules with sizes of 200–500 nm in methanol–water mixtures.[54] Ryadnov and coworkers showed that trigonal tryptophan zipper-forming peptide conjugate was useful as a nucleic acid carrier.[55] Woolfson and coworkers demonstrated that two complementary hubs comprising coiled-coil bundles self-assembled into uni-lamellar spheres with sizes of about 100 nm.[56]

6. Artificial Viral Capsids Self-assembled from β-Annulus Peptide

Recently, the application of bacteriophages such as M13 phage and plant viruses, including cowpea mosaic virus (CPMV) and cowpea chlorotic mottle virus (CCMV), to nanotechnology has attracted much attention due to their fascinating nanostructures.[57-61] These virus-based nanotechnologies depend on the structure of "ready-made" capsids; however, chemical strategies to rational design of artificial viral capsids are still in their infancy. As described above, the self-assembly of trigonal peptide conjugates afforded nanospheres, but it is difficult to modify the surface and interior selectively. If virus-like nanocapsules can be constructed from peptide fragments containing subunits of viral capsids, the peptide fragments would be promising candidates as components of chemically designable artificial nano-assemblies.

Tomato bushy stunt virus (TBSV) capsid comprises 180 quasi-equivalent protein subunits that comprise 388 amino acids each, in which the β-annulus motif participates in the formation of a dodecahedral internal skeleton.[1, 62] In 2010, we found that 24-mer β-annulus peptides (INHVGGTGGAIMAPVAVTRQL VGS) of TBSV spontaneously self-assembled into hollow nanocapsules with sizes of 30–50 nm in water (Figure 8A-C).[63] Small-angle X-ray scattering clearly indicated that the β-annulus peptide forms a hollow nanocapsule structure with an inner diameter of 36 nm and an outer diameter of 50 nm in aqueous

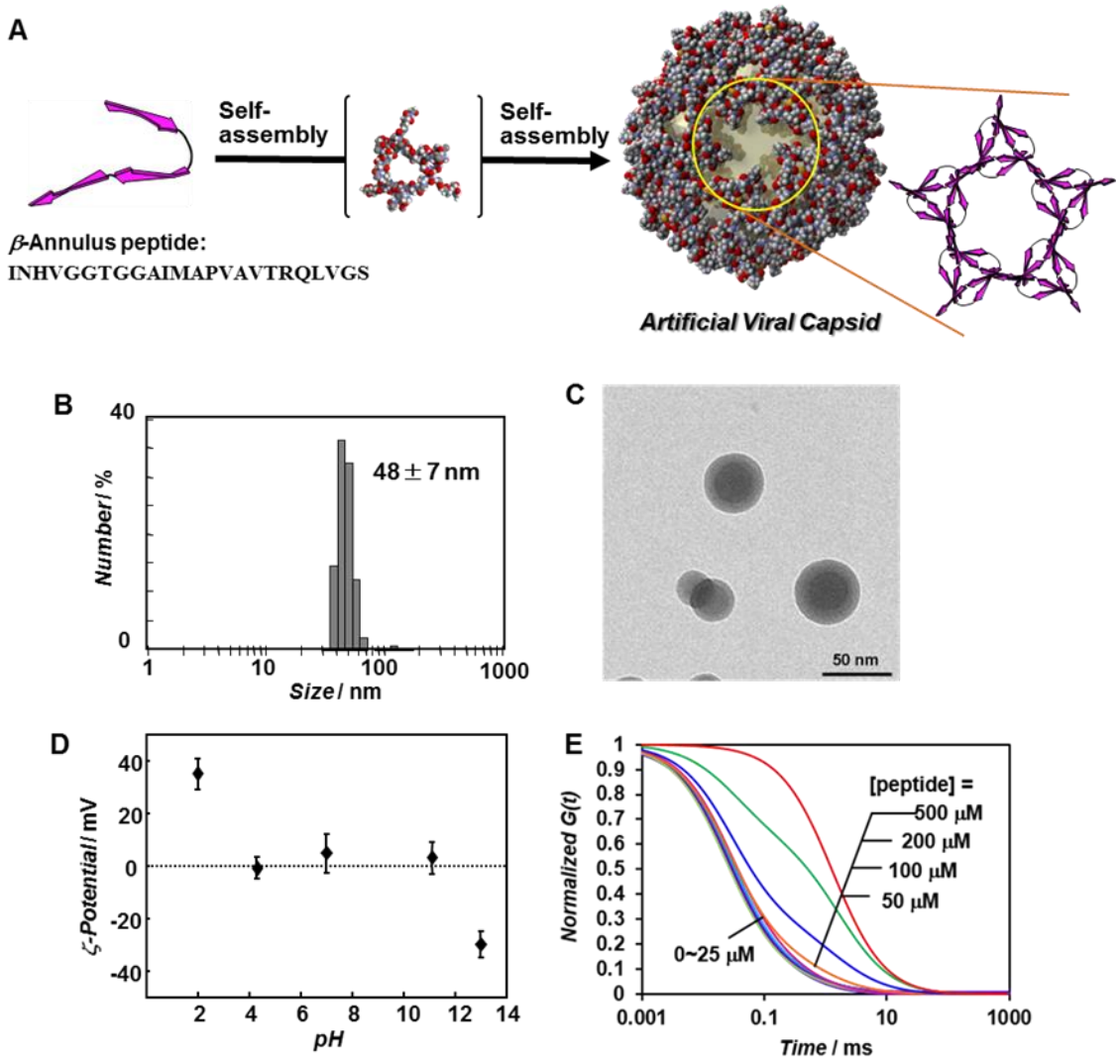

Figure 8. (A) Schematic illustration of the formation of artificial viral capsids by self-assembly of *β*-annulus peptide from TBSV. (B) Size distribution of the artificial viral capsids obtained from DLS. (C) TEM image of the artificial viral capsids. (D) Effect of pH on the *ζ*-potentials of the artificial viral capsids. (E) FCS analysis of encapsulation of CdTe quantum dots into the artificial viral capsids.

solution. It seems very interesting that only the 24-mer *β*-annulus peptide fragment from TBSV formed a spherical structure without forming a unimolecular folded structure or fiber structure. The artificial viral capsid possesses a definite critical aggregation concentration (CAC = 25 μM), and its size is almost unaffected by peptide concentration above the CAC. Other *β*-annulus peptides from SeMV also self-assembled into nanocapsule structures with sizes of about 30 nm.[64]

Figure 8D shows the pH dependence of the *ζ*-potential of the artificial viral capsids, which indicates that the surface *ζ*-potentials of the artificial viral capsids are dominated by the charges of the C-terminal sequence (RQLVGS-COOH), and the N-terminal sequence (H_2N-INH) has a minimal effect.[65] These results suggest that the C-terminal is directed to the outer surface, whereas the N-terminal is directed to the interior of the artificial capsids, which corresponds to the terminal-direction of the natural TBSV capsid. Thus, it is suggested that the outer surface of the artificial viral capsid is zwitterionic and the inside is cationic at neutral pH; therefore, it is considered that anionic molecules can be encapsulated inside. When encapsulation of various dyes in the artificial viral capsids was examined, it was found that anionic dyes were encapsulated without affecting the capsid structure. Polyanionic M13 phage DNA was also encapsulated in the artificial viral capsids. TEM observation of the DNA/*β*-annulus peptide complexes stained with cisplatin, which selectively binds to DNA, and uranyl acetate showed the formation of core–shell nanospheres of compacted DNA in peptide shells. To analyze *in situ* the encapsulation behavior of anionic nanoparticles into the artificial viral capsids in water, fluorescence correlation spectroscopy (FCS) of fluorescence CdTe quantum dots (3 nm) in the presence of *β*-annulus peptide was measured.[66] Figure 8E shows the normalized autocorrelation function curve of the CdTe quantum dots in the presence of various concentrations of *β*-annulus peptide. At concentrations below 25 μM, the autocorrelation function showed a single-component curve with a diffusion time of about 0.08 ms. At concentrations in the range 50−200 μM, the autocorrelation function showed a two-step decay curve, indicating the co-existence of fast and slow components. At 500 μM, the autocorrelation function curve was fitted to a single-component model comprising only a slow component with a diffusion time of 1.31 ms. These results indicate that CdTe quantum dots were encapsulated into the artificial viral capsids at concentrations above 50 μM, which corresponds to the CAC of the peptide.

As described above, it was suggested that the C-terminals

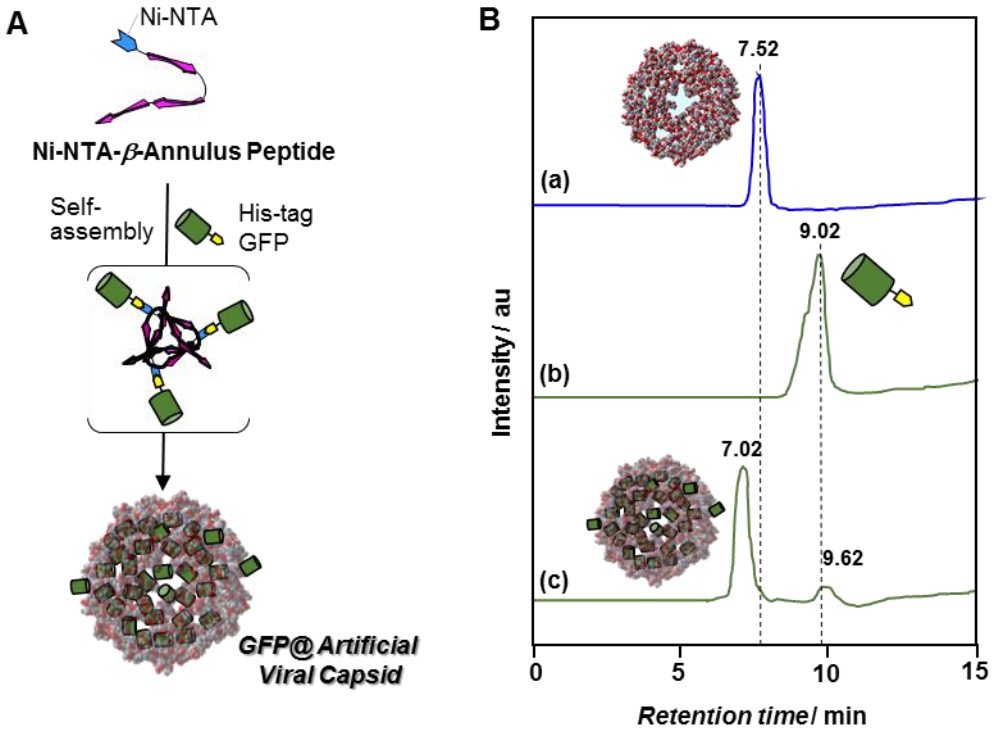

Figure 9. (A) Schematic illustration of encapsulation of His-tagged GFP into artificial viral capsids self-assembled from Ni-NTA-modified β-annulus peptide. (B) Size-exclusion chromatograph of (a) assemblies of Ni-NTA-modified β-annulus peptide, (b) His-tagged GFP alone, and (c) equimolar mixtures of His-tagged EGFP and Ni-NTA-modified β-annulus peptide.

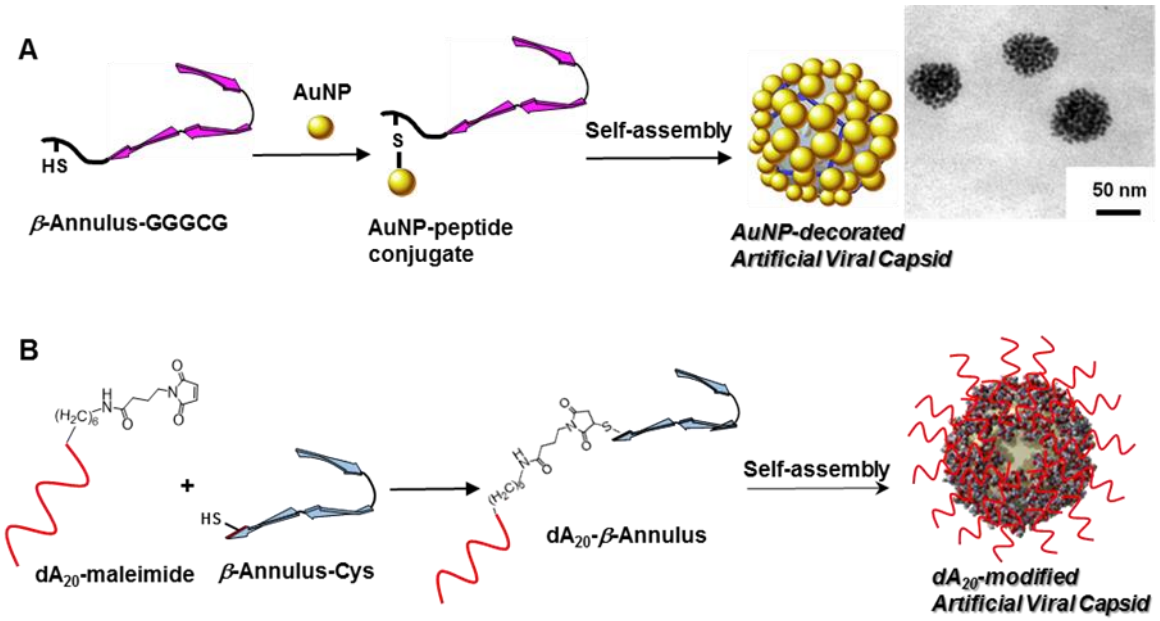

Figure 10. Surface decoration of artificial viral capsids with gold nanoparticles (A) and single-strand DNA (B).

of β-annulus peptides are directed toward the outer surface of artificial viral capsids, whereas the N-terminals are directed toward the interior. These properties enabled selective modification of the inner space of the artificial viral capsids by N-terminal modification of the β-annulus peptide. To encapsulate His-tagged proteins into the artificial viral capsids, β-annulus peptide modified with Ni-NTA (nitrilotriacetic acid) at the N-terminal was synthesized by the reaction of Cys of β-annulus peptide at the N-terminal with the maleimide derivative of NTA.[67] The Ni-NTA-modified β-annulus peptide self-assembled into artificial viral capsids with sizes of about 40 nm, which had a 470 times lower CAC than that of unmodified β-annulus peptides. Mixing the Ni-NTA-modified β-annulus peptide and equimolar His-tagged green fluorescence protein (His-tag GFP) afforded GFP-encapsulated artificial viral capsids with sizes of 50 nm (Figure 9A). SEC of equimolar mixtures of His-tag GFP and Ni-NTA-modified artificial viral capsid showed two elution peaks, reflecting 91% encapsulation of GFP in the artificial viral capsids and 9% free GFP, respectively (Figure 9B). Similarly, fluorescence ZnO nanoparticles were encapsulated in

the artificial viral capsids self-assembled from β-annulus peptide bearing a ZnO-binding sequence (HCVAHR) at the N-terminal.[68]

To decorate the artificial viral capsids with functional molecules, the C-terminal of β-annulus peptides were modified with 5 nm gold nanoparticles (AuNP) [69] and ODNs (dA_{20} and dT_{20}).[70] AuNP–β-annulus peptide conjugate was prepared by mixing Cys-containing β-annulus peptide at the C-terminal with AuNPs at a concentration below the CAC followed by protection with thioctic acid. After concentrating to above the CAC, TEM images of the AuNP–β-annulus peptide conjugate showed the formation of AuNP assemblies with diameters of 30–60 nm (Figure 10A). The ζ-potential of the AuNP assemblies at pH 4.6 was −30.5 ± 9.8 mV, whereas that of unmodified artificial viral capsids at the same pH was 0.01 ± 9.8 mV. These results indicate that AuNPs decorated the outer surface of the artificial viral capsids. ODN-conjugated β-annulus peptides were prepared by the reaction of Cys of β-annulus peptide at the C-terminal with maleimide-modified ODNs (dA_{20} and dT_{20}). The ODN-conjugated β-annulus peptides self-assembled into artificial viral capsids with sizes of 45–160 nm, despite anionic repulsion (Figure 10B). The dA_{20}-modified artificial viral capsids formed aggregates upon addition of complementary polynucleotides (poly-dT). The present strategy for surface decoration of artificial viral capsids could be extended to the creation of artificial viral capsids modified with enzymes, receptor proteins, antigens, and so on.

7. Conclusion

This account article gave an overview of our research on the construction of supramolecules by self-assembly of rationally designed biomolecules. Various biomaterials with useful functions have been developed by proper design of DNAs and peptides. These self-assembled biomaterials could be applied to novel drug carriers, nano-templates, ligand-displaying scaffolds, and as a platform for vaccines. I envisage that artificial dynamic nano-machine systems could be developed by self-organization of designed biomolecules in the future.

Acknowledgement

I would like to thank Emeritus Prof. Kazukiyo Kobayashi (Nagoya University), Prof. Nobuo Kimizuka (Kyushu University), and all the co-worker whose names are cited in the references for their valuable contribution. This work financially supported by PRESTO, Japan Science and Technology Agency, Japan Society for the Promotion of Science (JSPS), and the Ministry of Education, Culture, Science, Sports and Technology of Japan.

References

1. C. Branden, J. Tooze, *Introduction to Protein Structure*, 2nd edition, Garland Publishing, New York, **1999**.
2. C. M. Niemeyer, C. A. Mirkin (Eds.), *Nanobiotechnology*, Wiley-VCH, Weinheim, **2004.**
3. C. A. Mirkin, C. M. Niemeyer (Eds.), *Nanobiotechnology II*, Wiley-VCH, Weinheim, **2007.**
4. E. Stulz, G. H. Clever (Eds.), *DNA in Supramolecular Chemistry and Nanotechnology*, Wiley, Weinheim, **2015**.
5. C. Aleman, A. Bianco, M. Venanzi (Eds.), *Peptide Materials: From Nanostuctures to Applications*, Wiley, Weinheim, **2013**.
6. M. Mammen, S.Choi, G. M. Whitesides, *Angew. Chem. Int. Ed*. **1998**, *37*, 2754.
7. C. Fasting, C. A. Schalley, M. Weber, O. Seitz, S. Hecht, B. Koksch, J. Dernedde, C. Graf, E.-W. Knapp, R. Haag, *Angew. Chem. Int. Ed.* **2012**, *51*, 10472.
8. J. J. Lundquist, E. J. Toone, *Chem. Rev.* **2002**, 102, 555.
9. Y. Miura, Y. Hoshino, H. Seto, *Chem. Rev.* **2016**, *116*, 1673.
10. T. Hasegawa, S. Kondoh, K. Matsuura, K. Kobayashi, *Macromolecules* **1999**, *32*, 6595.
11. Y. Ohya, K. Yabuki, M. Hashimoto, A. Nakajima, T. Ouchi, *Bioconj. Chem.* **2003**, *14*, 1057.
12. K. Matsuura, M. Hibino, M. Kataoka, Y. Hayakawa, K. Kobayashi, *Tetrahedron Lett.* **2000**, *41*, 7529.
13. K. Matsuura, M. Hibino, Y. Yamada, K. Kobayashi, *J. Am. Chem. Soc.* **2001**, *123*, 357.
14. K. Matsuura, M. Hibino, T. Ikeda, Y. Yamada, K. Kobayashi, *Chem. Eur. J.* **2004**, *10*, 352.
15. Y. Yamada, K. Matsuura, and K. Kobayashi, *Bioorg. Med. Chem.* **2005**, *13*, 1913.
16. T. Akasaka, K. Matsuura, K. Kobayashi, *Bioconj. Chem.* **2001**, *12*, 776.
17. C. Scheibe, A. Bujotzek, J. Dernedde, M. Weber, O. Seitz, *Chem. Sci.* **2011**, *2*, 770.
18. C. Scheibe, O. Seitz, *Pure Appl. Chem.* **2012**, *84*, 77.
19. H. Eberhard, F. Diezmann, O. Seitz, *Angew. Chem. Int. Ed.* **2011**, *50*, 4146.
20. J. D'Onofrio, L. Petraccone, L. Martino, G. D. Fabio, A. Iadonisi, J. Balzarini, C. Giancola, D. Montesarchio, *Bioconjugate Chem.* **2008**, *19*, 607.
21. B. A. Rosenzweig, N. T. Ross, D. M. Tagore, J. Jayawickramarajah, I. Saraogi, A. D. Hamilton, *J. Am. Chem. Soc.* **2009**, *131*, 5020.
22. M. Matsui, Y. Ebara, *Bioorg. Med. Chem. Lett.* **2012**, *22*, 6139.
23. H. Asanuma, D. Tamaru, A. Yamazawa, M. Liu, M. Komiyama, *ChemBioChem* **2002**, *3*, 786.
24. Y. Katayama, K. Fujii, E. Ito, S. Sakakihara, T. Sonoda, M. Murata, M. Maeda, *Biomacromolecules* **2002**, *3*, 905.
25. K. Matsuura, K. Hayashi, K. Kobayashi, *Chem. Commun.* **2002**, *10*, 1140.
26. K. Matsuura, K. Hayashi, K. Kobayashi, *Biomacromolecules* **2005**, *6*, 2533.
27. K. Matsuura, T. Akasaka, M. Hibino, K. Kobayashi, *Bioconj. Chem.* **2000**, *11*, 202.
28. T. Akasaka, K. Matsuura, N. Emi, K. Kobayashi, *Biochem. Biophys. Res. Commun.* **1999**, *260*, 323.
29. J. Chen, N. C. Seeman, *Nature* **1991**, *350*, 631.
30. N. C. Seeman, *Nature* **2003**, *421*, 427.
31. P. W. K. Rothemund, *Nature* **2006**, *440*, 297.
32. J. Nangreave, D. Han, Y. Liu, H. Yan, *Curr. Opin. Chem. Biol.* **2010**, *14*, 608.
33. K. Matsuura, T. Yamashita, Y. Igami, N. Kimizuka, *Chem. Commun.* **2003**, 376.
34. K. Kim, K. Masumoto, K. Matsuura, N. Kimizuka, *Chem. Lett.* **2006**, *35*, 486.
35. K. Matsuura, K. Masumoto, Y. Igami, T. Fujioka, N. Kimizuka, *Biomacromolecules* **2007**, *8*, 2726.
36. K. Matsuura, K. Masumoto, Y. Igami, K. Kim, N. Kimizuka, *Mol. BioSys.* **2009**, *5*, 921.
37. K. Kim, K. Matsuura, N. Kimizuka, *Bioorg. Med. Chem.* **2007**, *15*, 4311.
38. K. Matsuurua, *RSC Adv.* **2014**, *4*, 2942.
39. B. E. I. Ramakers, J. C. M. van Hesta, D. W. P. M. Löwik, *Chem. Soc. Rev*. **2014**, *43*, 2743.
40. E. D. Santis, M. G. Ryadnov, *Chem. Soc. Rev*. **2015**, *44*, 8288.
41. Q. Luo, C. Hou, Y. Bai, R. Wang, J. Liu, *Chem. Rev.* **2016**, *116*, 13571.
42. J. C. T. Carlson, S. S. Jena, M. Flenniken, T. F. Chou, R. A. Siegel, C. R. Wagner, *J. Am. Chem. Soc.* **2006**, *128*, 7630.

43. J. E. Padilla, C. Colovos, T. O. Yeates, *Proc. Nat. Acad. Sci., USA* **2001**, *98*, 2217.
44. Y. T. Lai, K. L. Tsai, M. R. Sawaya, F. J. Asturias, T. O. Yeates, *J. Am. Chem. Soc.* **2013**, *135*, 7738.
45. Y. T. Lai, E. Reading, G. L. Hura, K.-L. Tsai, A. Laganowsky, F. J. Asturias, J. A. Tainer, C. V. Robinson, T. O. Yeates, *Nat. Chem.* **2014**, *6*, 1065.
46. K. Matsuura, K. Murasato, N. Kimizuka, *J. Am. Chem. Soc.* **2005**, *127*, 10148.
47. K. Murasato, K. Matsuura, N. Kimizuka, *Biomactromolecules* **2008**, *9*, 913.
48. K. Matsuura, H. Hayashi, K. Murasato, N. Kimizuka, *Chem. Commun.* **2011**, *47*, 265.
49. K. Matsuura, K. Murasato N. Kimizuka, *Int. J. Mol. Sci.* **2011**, *12*, 5187.
50. R. P. Lyon, W. M. Atkins, *J. Am. Chem. Soc.* **2001**, *123*, 4408.
51. K. Matsuura, H. Matsuyama, T. Fukuda, K. Murasato, N. Kimizuka, *Soft Matter* **2009**, *5*, 2463.
52. K. Matsuura, K. Tochio, K. Watanabe, N. Kimizuka, *Chem. Lett.* **2011**, *40*, 711.
53. K. Matsuura, K. Fujino, T. Teramoto, K. Murasato, N. Kimizuka, *Bull. Chem. Soc. Jpn.* **2010**, *83*, 880.
54. S. Ghosh, M. Reches, E. Gazit, S. Verma, *Angew. Chem. Int. Ed.* **2007**, *46*, 2002.
55. V. Castelletto, E. D. Santis, H. Alkassem, B. Lamarre, J. E. Noble, S. Ray, A. Bella, J. R. Burns, B. W. Hoogenboom, M. G. Ryadnov, *Chem. Sci.* **2016**, *7*, 1707.
56. J. M. Fletcher, R. L. Harniman, Fr. R. H. Barnes, A. L. Boyle, A. Collins, J. Mantell, T. H. Sharp, M. Antognozzi, P. J. Booth, N. Linden, M. J. Miles, R. B. Sessions, P. Verkade, D. N. Woolfson, *Science* **2013**, *340*, 595.
57. T. Douglas, M. Young, *Science* **2006**, *312*, 873.
58. M. Uchida, M. T. Klem, M. Allen, P. Suci, M. Flenniken, E. Gillitzer, Z. Varpness, L. O. Liepold T. Douglas M. Young, *Adv. Mater.* **2007**, *19*, 1025.
59. N. F. Steinmetz, D. J. Evans, *Org. Biomol. Chem.* **2007**, *5*, 2891.
60. L. M. Bronstein, *Small* **2011**, *7*, 1609.
61. L. S. Witus, M. B. Francis, *Acc. Chem. Res.* **2011**, *44*, 774.
62. J. Olson, G. Bricogne, S. C. Harrison, *J. Mol. Biol.* **1983**, *171*, 61.
63. K. Matsuura, K. Watanabe, K. Sakurai, T. Matsuzaki, N. Kimizuka, *Angew. Chem. Int. Ed.* **2010**, *49*, 9662.
64. K. Matsuura, Y. Mizuguchi, N. Kimizuka, *Biopolymers: Pept. Sci.* **2016**, *106*, 470.
65. K. Matsuura, K. Watanabe, Y. Matsushita, N. Kimizuka, *Polymer J.* **2013**, *45*, 529.
66. S. Fujita, K. Matsuura, *Chem. Lett.* **2016**, *45*, 922.
67. K. Matsuura, T. Nakamura, K. Watanabe, T. Noguchi, K. Minamihata, N. Kamiya, N. Kimizuka, *Org. Biomol. Chem.* **2016**, *14*, 7869.
68. S. Fujita, K. Matsuura, *Nanomaterials* **2014**, *4*, 778.
69. K. Matsuura, G. Ueno, S. Fujita, *Polymer J.* **2015**, *47*, 146.
70. Y. Nakamura, S. Yamada, S. Nishikawa, K. Matsuura, *J. Pept. Sci.* **2017**, DOI: 10.1002/psc.2967.

Graphical Abstract

Construction of Functional Biomaterials by Biomolecular Self-assembly

K. Matsuura

<Summary>
This account discusses construction strategies for various functional biomaterials, such as novel glycoclusters along DNA, nucleospheres, and virus-like peptide nanospheres, based on the designed self-assembly of biomolecules.

<Diagram>